MNRAS 000, 1–24 (2018) Preprint 10 May 2019 Compiled using MNRAS LATEX style file v3.0

The Effects of Diffuse Ionized Gas and Spatial Resolution on Metallicity Gradients: TYPHOON Two-Dimensional Spectrophotometry of M83

Henry Poetrodjojo[1,2,★] Joshua J. D'Agostino[1,2], Brent Groves[1,2], Lisa Kewley[1,2], I-Ting Ho[3], Jeff Rich[4], Barry F. Madore[4] and Mark Seibert[4]

[1]*Research School of Astronomy and Astrophysics, The Australian National University, Cotter Road, Weston, ACT 2611, Australia*
[2]*ARC Centre of Excellence for All Sky Astrophysics in 3 Dimensions (ASTRO 3D)*
[3]*Max Planck Institute for Astronomy, Königstuhl 17, 69117 Heidelberg, Germany*
[4]*Observatories of the Carnegie Institution of Washington, 813 Santa Barbara St, Pasadena, CA 91101, USA*

Accepted XXX. Received YYY; in original form ZZZ

ABSTRACT

We present a systematic study of the diffuse ionized gas (DIG) in M83 and its effects on the measurement of metallicity gradients at varying resolution scales. Using spectrophotometric data cubes of M83 obtained at the 2.5m duPont telescope at Las Campanas Observatory as part of the TYPHOON program, we separate the HII regions from the DIG using the [SII]/Hα ratio, HIIPHOT (HII finding algorithm) and the Hα surface brightness. We find that the contribution to the overall Hα luminosity is approximately equal for the HII and DIG regions. The data is then rebinned to simulate low-resolution observations at varying resolution scales from 41 pc up to 1005 pc. Metallicity gradients are measured using five different metallicity diagnostics at each resolution. We find that all metallicity diagnostics used are affected by the inclusion of DIG to varying degrees. We discuss the reasons of why the metallicity gradients are significantly affected by DIG using the HII dominance and emission line ratio radial profiles. We find that applying the [SII]/Hα cut will provide a closer estimate of the true metallicity gradient up to a resolution of 1005 pc for all metallicity diagnostics used in this study.

Key words: galaxies:abundances – galaxies:ISM – galaxies:individual (M83)

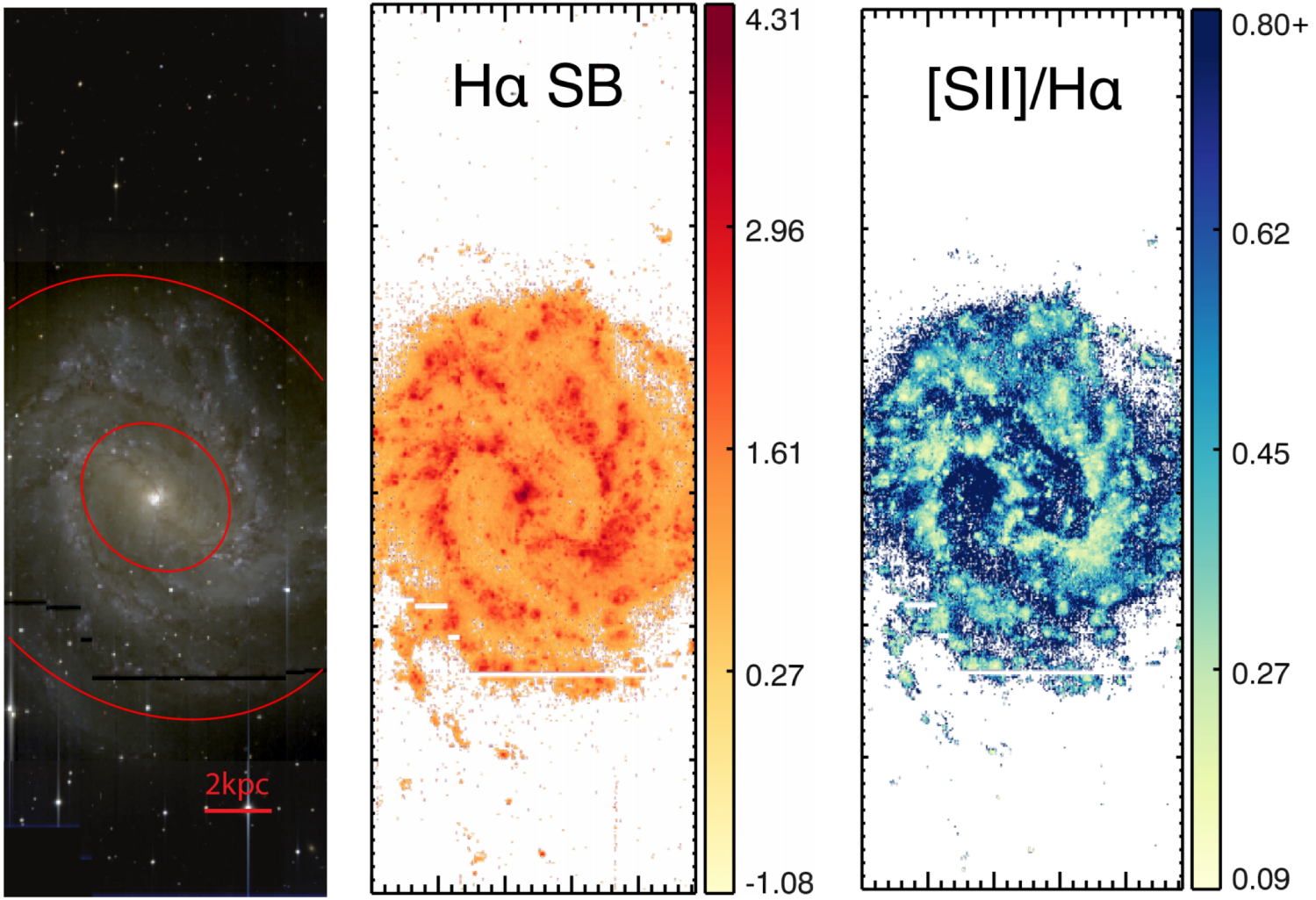

Figure 1. *Left*: BVR composite image of M83 created from the TYPHOON datacube. The two red ellipses correspond to 0.5 and 1.5 R_e of the galactic disk. *Middle*: Hα surface brightness map of M83 extracted by LZIFU in units of $\log(10^{-17}$ erg/s/cm^2/arcsec$^2)$. *Right*: The [SII]/Hα emission line ratio map of M83. Diffuse ionized gas is known to have increased emission line ratios such as [SII]/Hα and [NII]/Hα . As a result, [SII]/Hα is often used as a tracer for diffuse ionized gas.

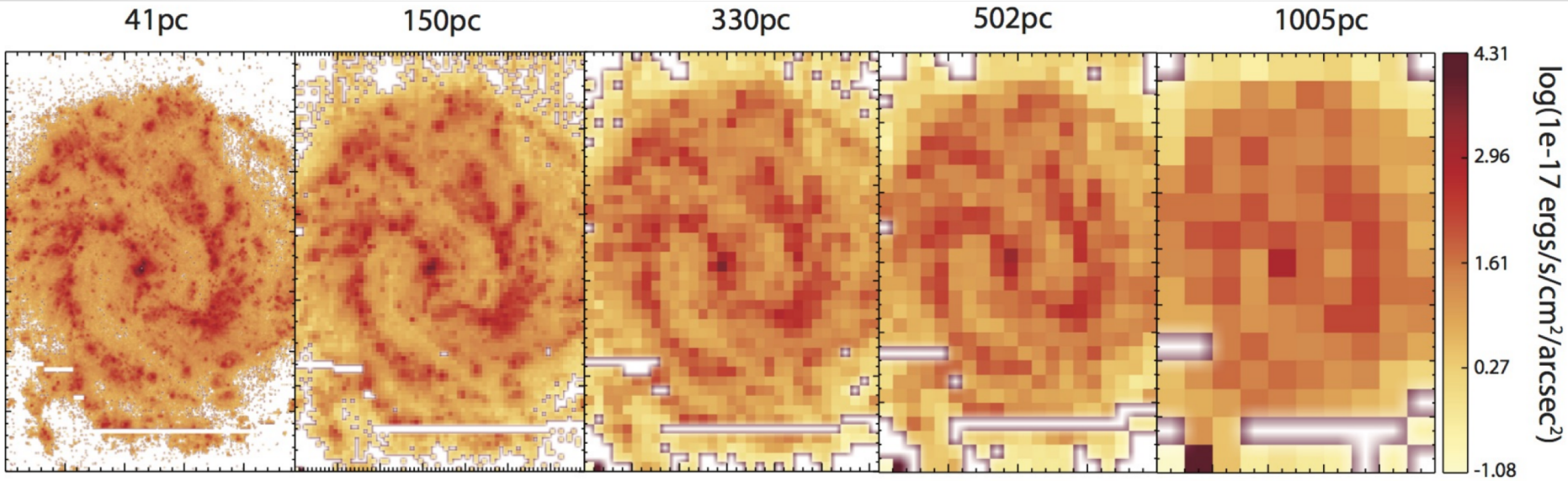

Figure 2. Hα map of M83 at different resolution scales. The spatial resolutions from left to right: 41 pc, 150 pc, 330 pc, 502 pc and 1005 pc. The gradual blurring of defined HII regions and the merging of the spiral arms with the inter-arm regions can be clearly seen in this figure.

Цель:

- Как DIG влияет на оценки металличности каждым методом?
- Какой метод менее всего чувствителен к DIG?
- Как все портится с ухудшением разрешения?

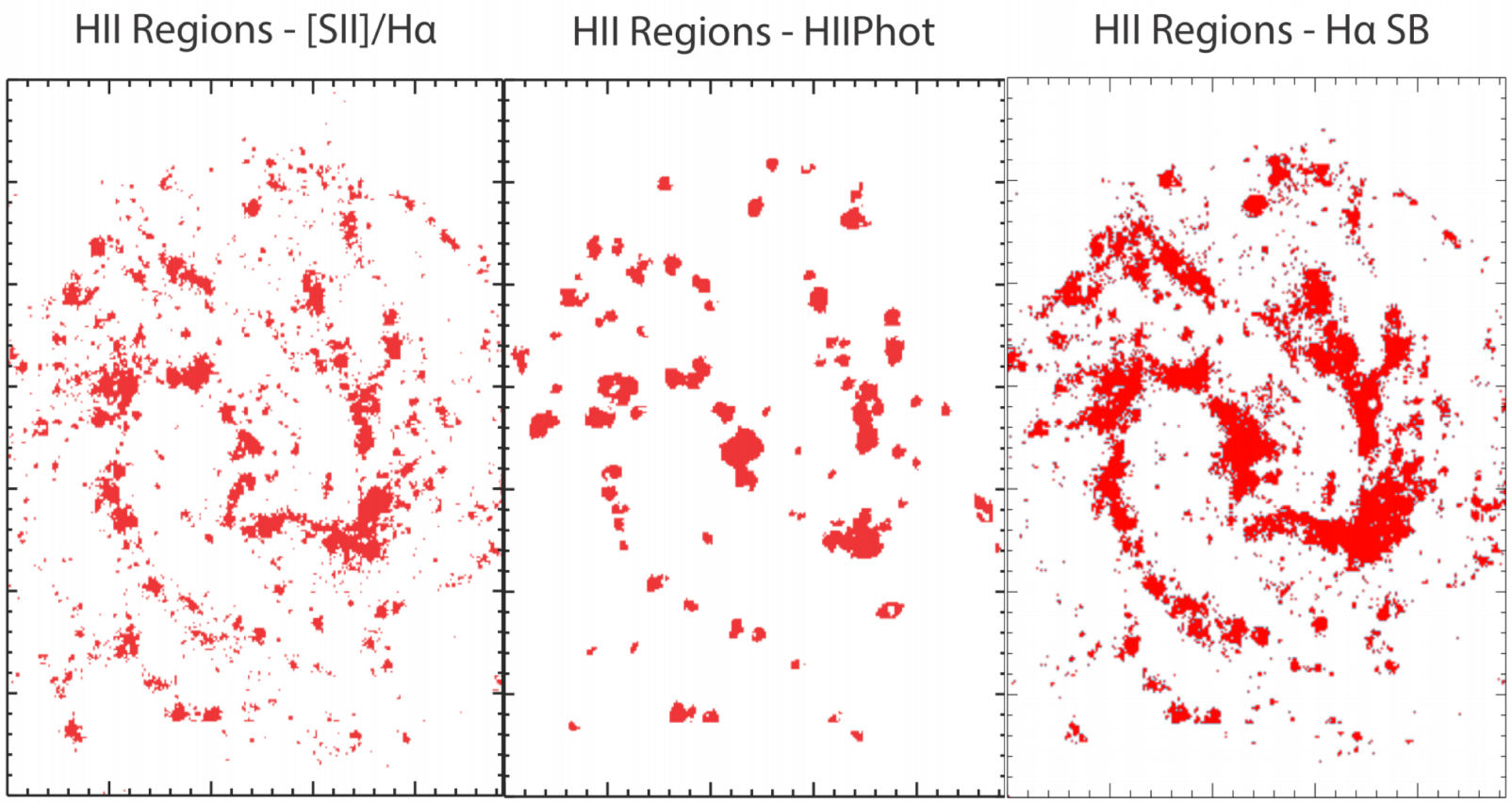

Figure 3. Maps of the three DIG classification schemes used in this paper. *Left*: HII region classification using the [SII]/Hα emission line ratio. [SII]/Hα < 0.29 is defined as HII regions and [SII]/Hα > 0.29 is defined as DIG. *Middle*: HII regions defined using a modified version of HIIPHOT (Thilker et al. 2000). HIIPHOT determines HII regions based on local Hα surface brightness profiles. *Right*: HII regions determined by a Hα surface brightness cut-off. Σ(Hα)> 1.86×10^{-15} erg s^{-1} cm^{-2} arcsec^{-2} is defined as HII regions with anything less being classified as DIG.

Утверждают, что [SII]/Ha лучше всего подходит для разделения DIG и HII

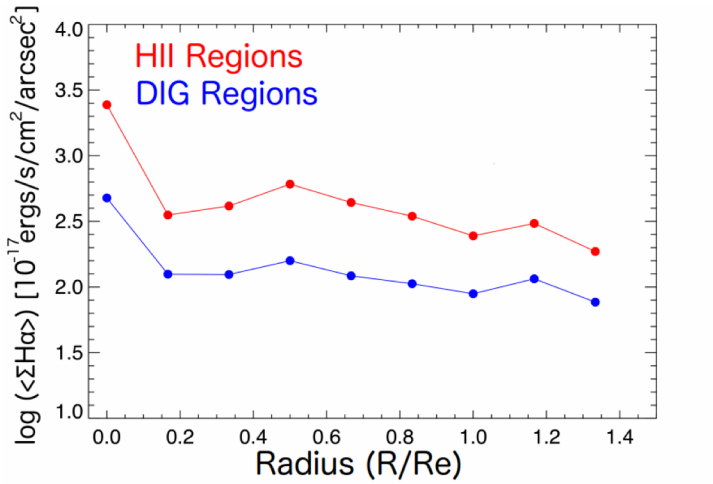

Figure 4. Radial Hα surface brightness profiles for HII regions and DIG regions using the [SII]/Hα HII classification scheme. The shape of the radial profiles look almost identical with the HII regions being significantly brighter than the DIG regions.

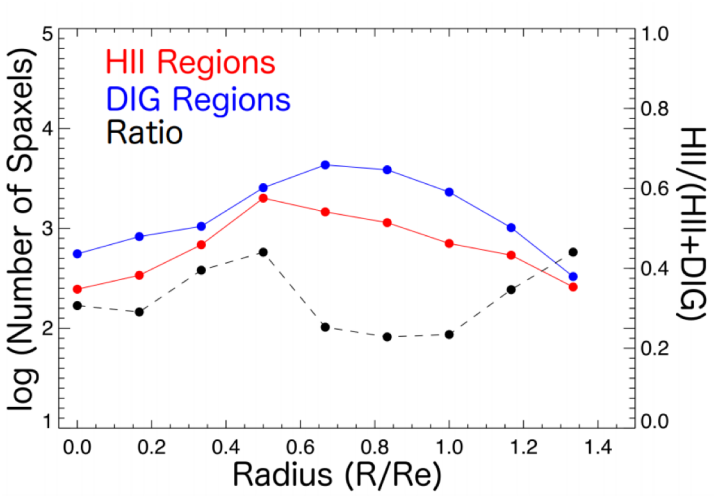

Figure 5. The number of spaxels classified as HII and DIG using the [SII]/Hα HII classification scheme. There are vastly more DIG spaxels than HII spaxels at all radii. The number of HII region spaxels peaks at $R/R_e = 0.6$, corresponding to the location of the spiral arms. The number of DIG spaxels steadily increases at larger radii due to the increase in area but flattens as detection of faint regions becomes difficult.

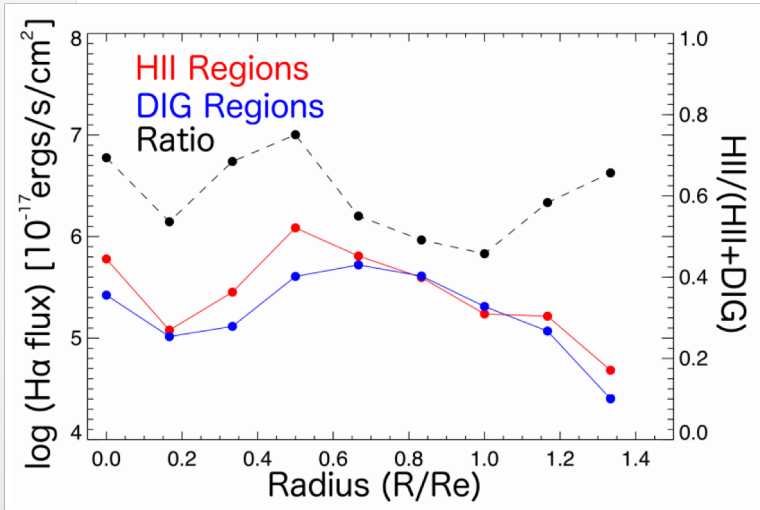

Figure 6. The Hα luminosity radial profile of M83. The luminosity profiles of HII and DIG regions are almost identical meaning that the total Hα luminosity is almost evenly contributed by HII regions and DIG regions. Even though HII regions are significantly brighter (Figure 4), there are far more DIG regions (Figure 5) to contribute to the luminosity.

Вклад DIG в общий поток Halpha сравним с вкладом от HII областей, особенно при плохом разрешении

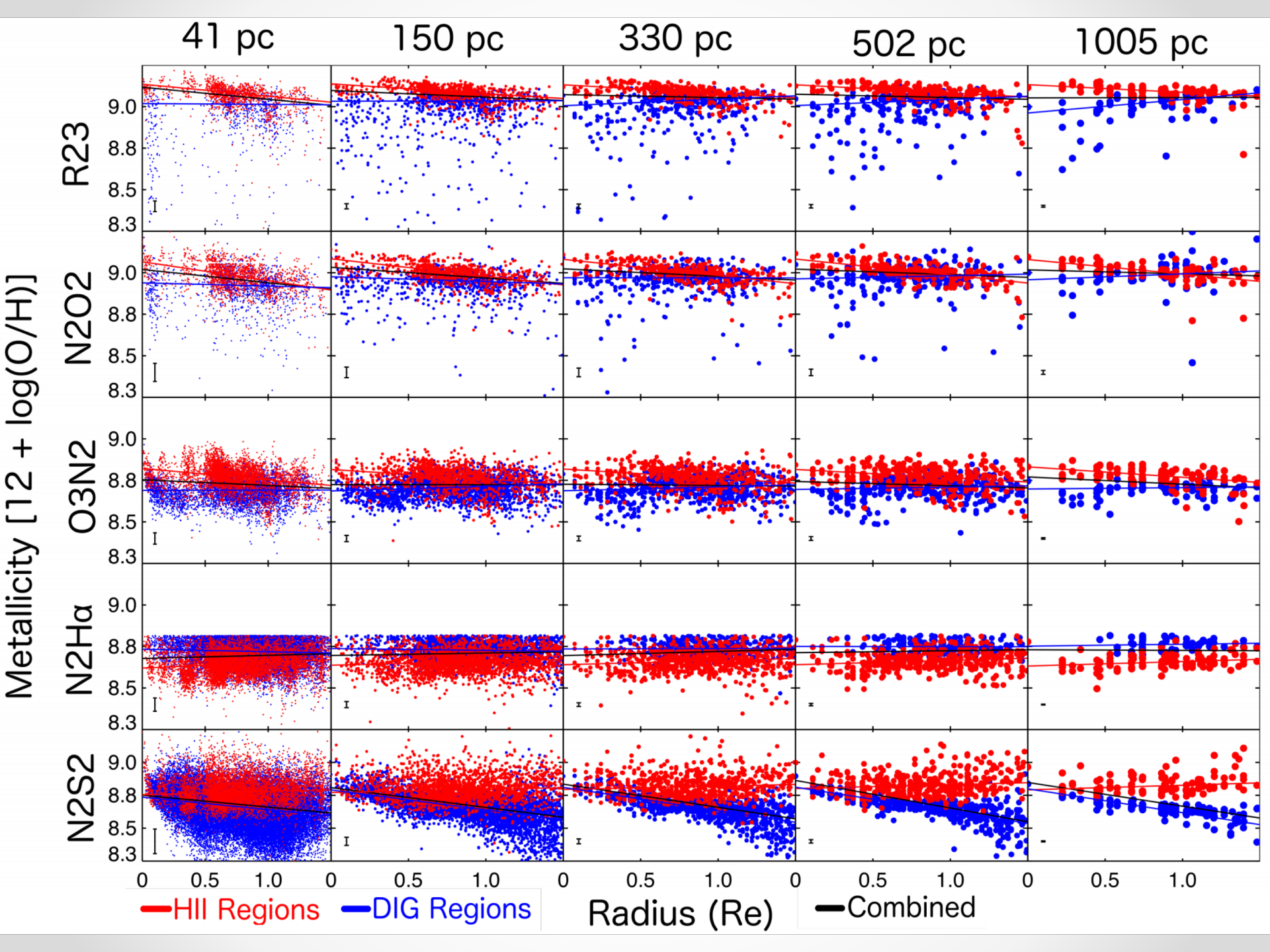
41 pc
150 pc
330 pc
502 pc
1005 pc
R23
N2O2
O3N2
N2Hα
N2S2
Metallicity [12 + log(O/H)]
9.0
8.8
8.5
8.3
0
0.5
1.0
HII Regions
DIG Regions
Radius (Re)
Combined

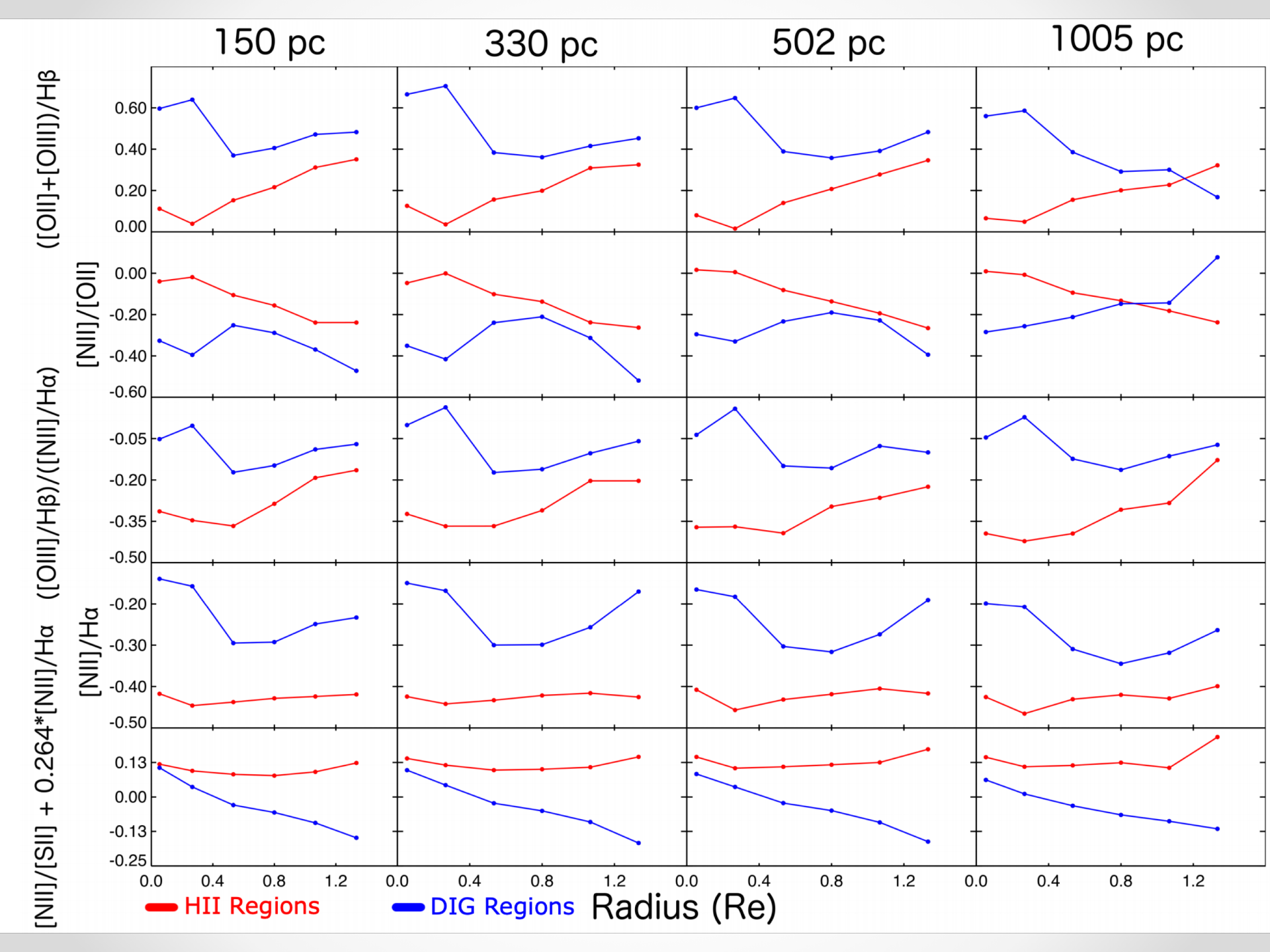
150 pc
330 pc
502 pc
1005 pc
([OII]+[OIII])/Hβ
[NII]/[OII]
([OIII]/Hβ)/([NII]/Hα)
[NII]/Hα
[NII]/[SII] + 0.264*[NII]/Hα
HII Regions
DIG Regions
Radius (Re)